SUPPORTING INFORMATION

First-in-class chemical probes against poly(ADP-ribose) glycohydrolase (PARG) inhibit DNA repair with differential pharmacology to olaparib.

Dominic I. James,[1,I] Kate M. Smith,[1,I] Allan M. Jordan,[1,*] Emma E. Fairweather,[1] Louise A. Griffiths,[1] Nicola S. Hamilton,[1] James R. Hitchin,[1] Colin P. Hutton,[1] Stuart Jones,[1] Paul Kelly,[1] Alison E. McGonagle,[1] Helen Small,[1] Alexandra I. J. Stowell,[1] Julie Tucker,[2,∞] Ian D. Waddell,[1] Bohdan Waszkowycz[1] and Donald J. Ogilvie.[1]

[1] Drug Discovery Unit, Cancer Research UK Manchester Institute, University of Manchester, Wilmslow Road, Manchester, M20 4BX, U.K.

[2] Structure and Biophysics, Discovery Sciences, AstraZeneca, Alderley Park, Macclesfield, Cheshire, SK10 4TG, UK

[∞]Current address: Northern Institute for Cancer Research, Paul O'Gorman Building, Newcastle University, Newcastle upon Tyne, NE2 4HH, UK

Supplementary Results.

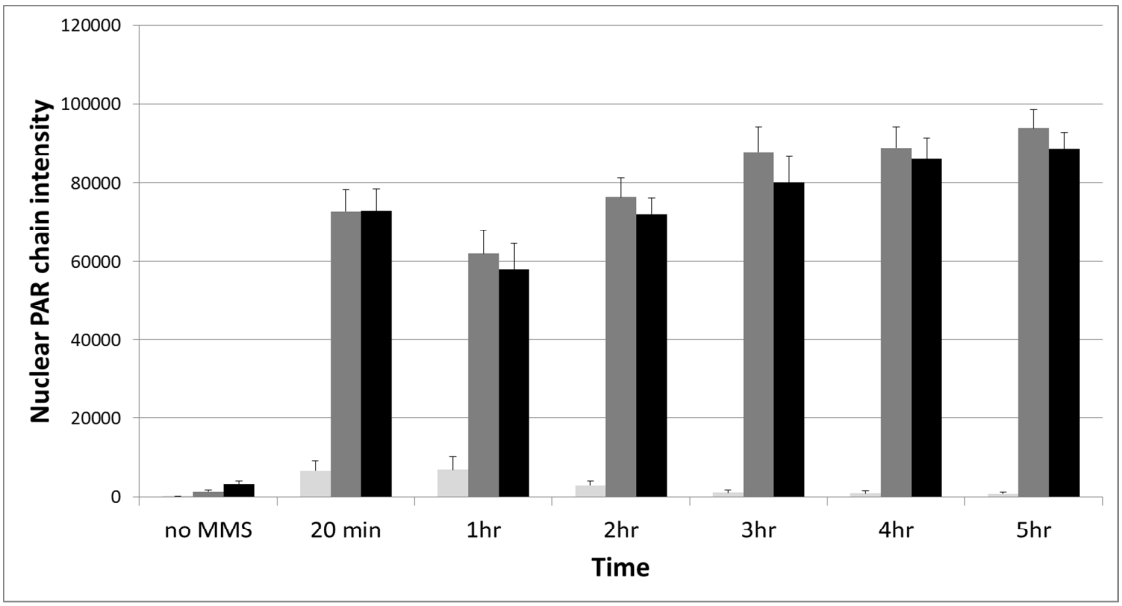

Supplemental Figure 1. PAR chains kinetics after PARG inhibition. 5 μM of PARG compounds **4** (black) or **5** (dark grey) or vehicle control (light grey) were added to HeLa cells for 1 hour. MMS was then added for differing amounts of time and the cells fixed and assayed for nuclear PAR chain intensity. PAR levels remain high for up to five hours after MMS addition. Error bars show standard deviation of triplicate values.

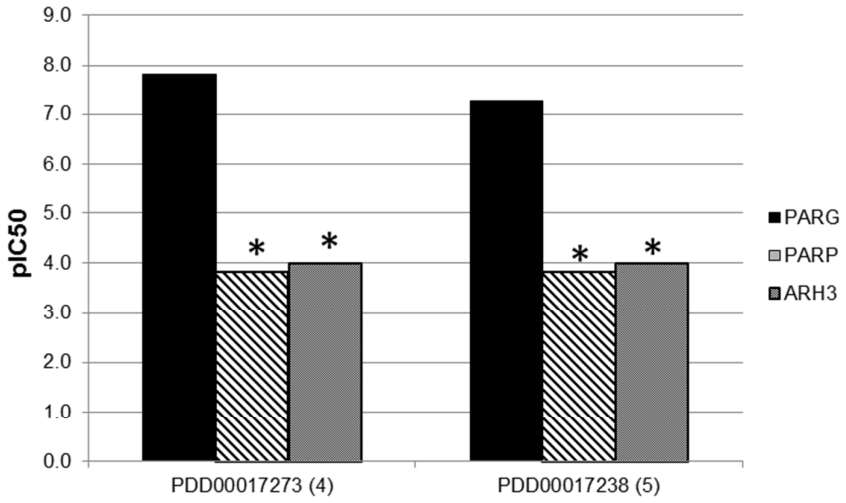

Supplemental Figure 2. PARG tool compounds are inactive against the related glycohydrolase ARH3 and PARP1. Compounds **4** (PDD00017273) and **5** (PDD00017238) were tested for their ability to inhibit PARP1 or ARH3 enzymes. The pIC_{50} values (defined as the negative logarithm of the IC_{50} value) are shown. An asterisk denotes that pIC_{50} values were lower the highest concentration tested (100 μM). Data is from four independent experiments.

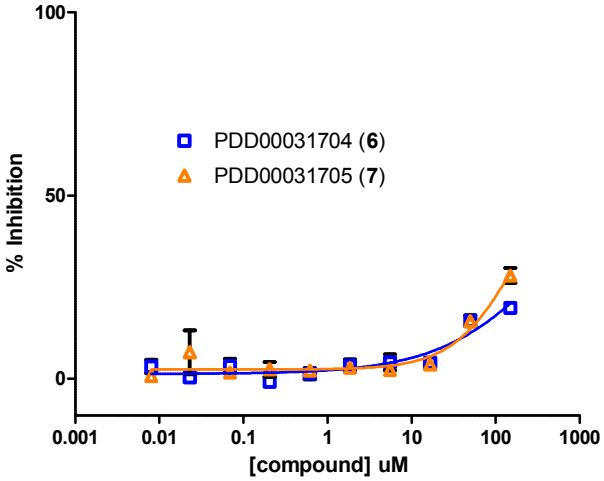

Supplemental Figure 3. N-methylated analogs of the PARG tool compounds are inactive. Compounds **6** (PDD00031704) and **7** (PDD00031705) were tested in the PARG biochemical assay and showed only low levels of PARG inhibition (< 50%) at high doses (> 100 μM). Error bars indicate s.e.m. from four experiments.

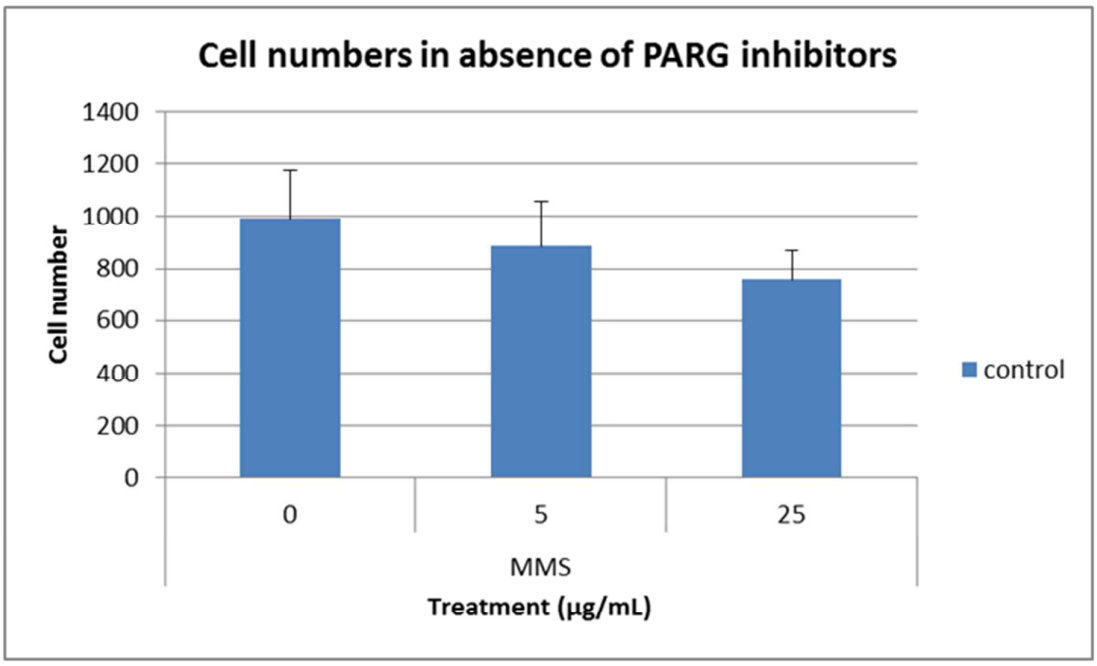

Supplemental Figure 4. MMS effect on MCF-7 cells after 24 h. MCF-7 cells were treated with DMSO (0) or different amounts of MMS for 24 h and cell number analysed after fixation and Hoechst-staining of nuclei. After 24 h, 5 µg mL^{-1} MMS led to a small but not significant decrease in cell number. Error bars indicate standard deviation from triplicate values and are representative of three experiments.

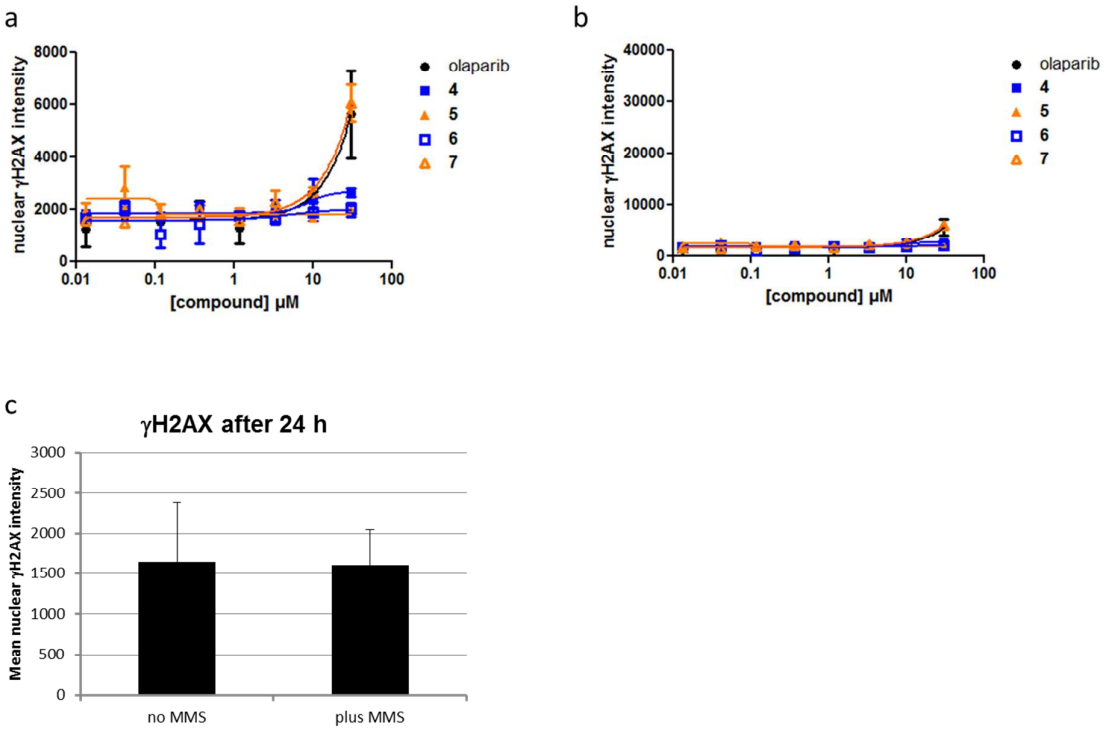

Supplemental Figure 5. γH2AX levels in MCF-7 cells. (a) After 24 h, in the absence of MMS, PARG inhibitors or olaparib have a minimal effect on γH2AX signal. Error bars indicate s.e.m. from four experiments. (b) The same values as in (a) with the y-axis scaled as in Figure 3a (main paper). (c) After 24 h in the presence of 5 μg mL^{-1} MMS, MCF-7 cells show no increase in γH2AX signal. Error bars indicate standard deviation from triplicate values and are representative of three experiments.

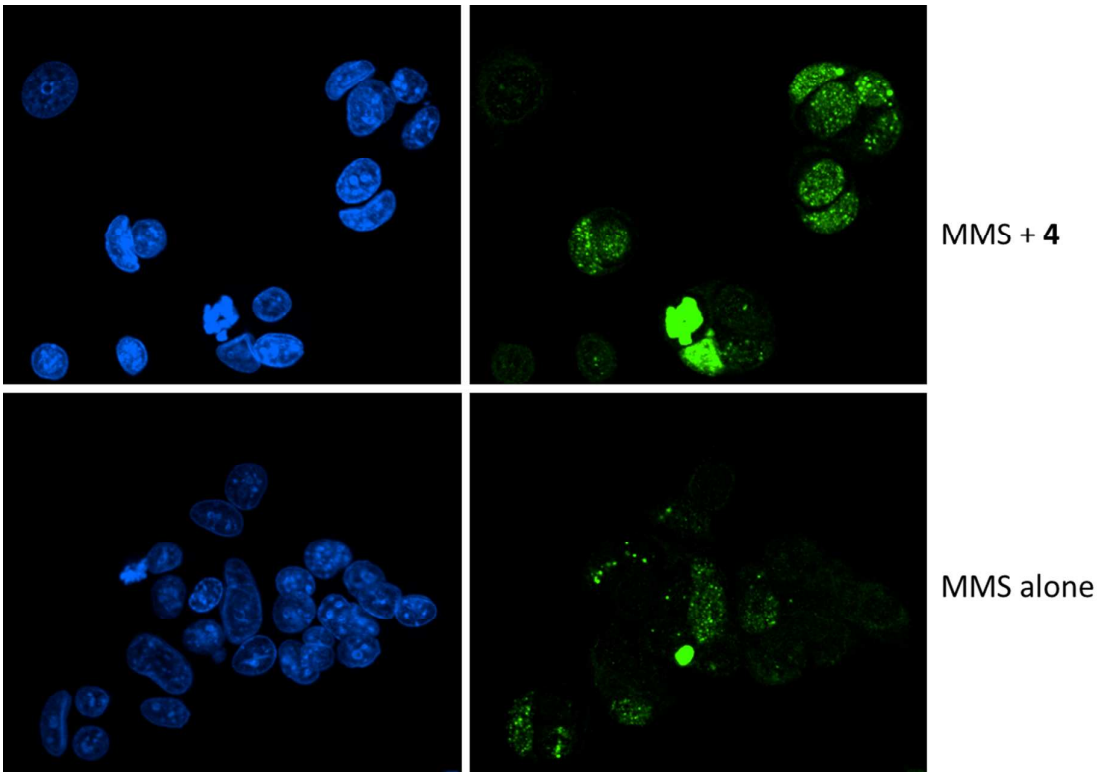

Supplemental Figure 6. PARG inhibitor enhances nuclear γH2AX staining. MCF-7 cells were treated with DMSO or **4** at 10 μM in the presence of 5 μg mL-1 of MMS for 24 h. After 24 h there is clear evidence that **4** increased pan-nuclear and punctate γH2AX staining in comparison to MMS alone.

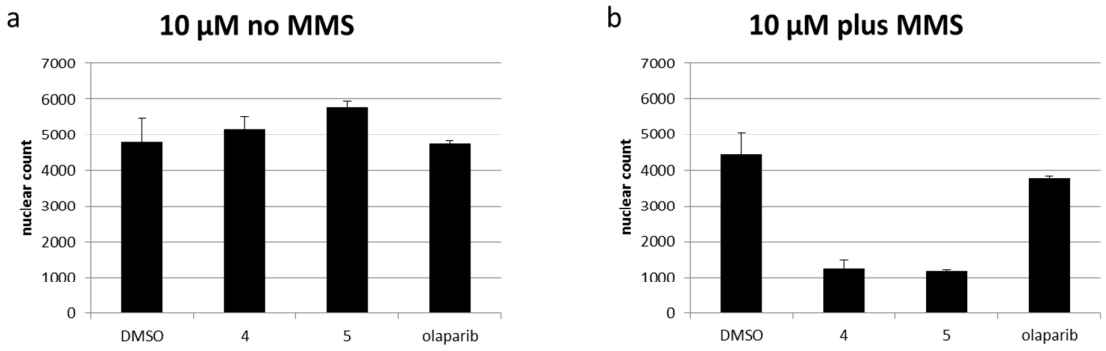

Supplemental Figure 7. Cell number after PARG or PARP inhibition in the presence or absence of MMS. (a) In MCF-7 cells, after 24 h, in the absence of MMS, PARG inhibitors or olaparib (both at 10 µM) have a minimal effect on proliferation. (b) In the presence of 5 µg mL^{-1} MMS, PARG inhibitors reduce cell number whilst the effect of olaparib on cell number is modest. Error bars indicate standard deviation from triplicate values and are representative of three experiments.

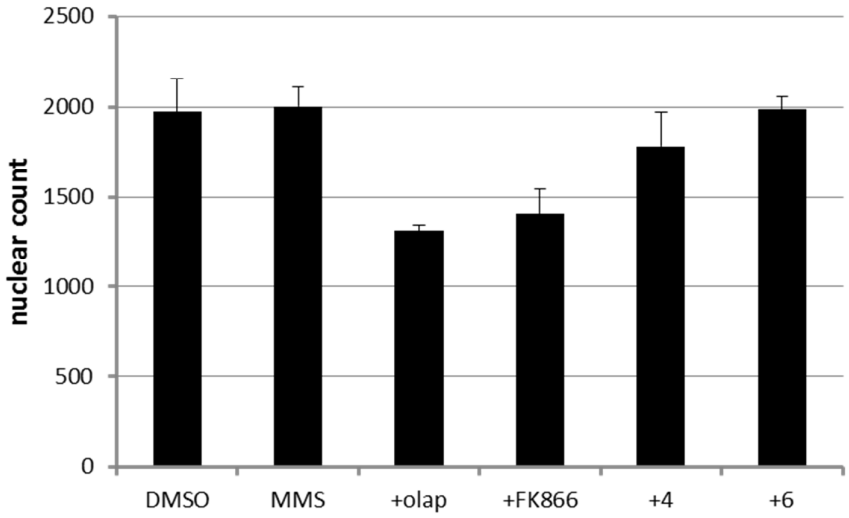

Supplemental Figure 8. Treatment with PARG or PARP inhibitor in combination with a low dose of MMS. HeLa cells were treated with DMSO or different inhibitors at 1 μM in the presence of 5 μg mL^{-1} of MMS for 24 h. After 24 h there is no decrease in cell number after treatment with 5 μg/mL MMS alone, whilst the combination of olaparib or FK866 with MMS decreased cell number more than the combination of active (**4**) or inactive (**6**) PARG inhibitor with MMS. Error bars indicate standard deviation from triplicate values and are representative of three experiments.

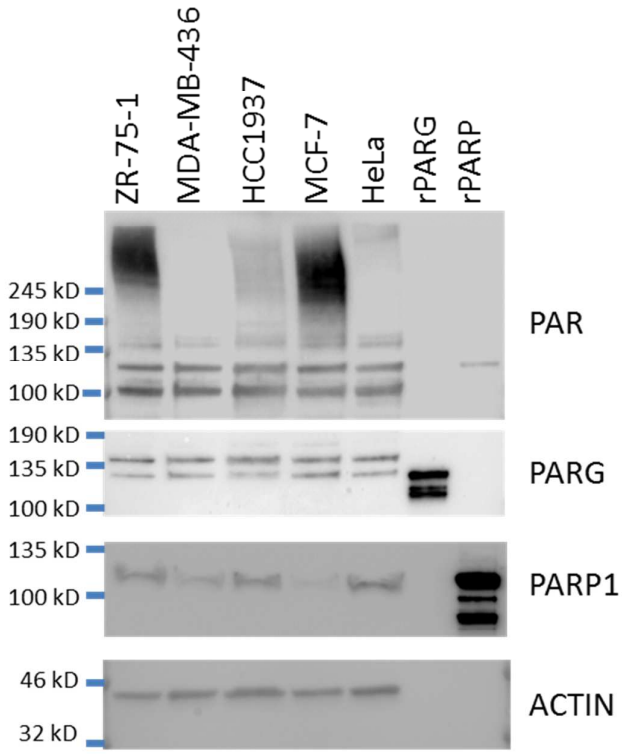

Supplemental Figure 9. Basal levels of PAR, PARG or PARP do not determine sensitivity. Breast cancer cell lines used in this study were examined for basal levels of PARG, PARP1 and PAR. ZR-75-1 cells had the highest levels of PAR and greatest sensitivity to PARG inhibition but lack of PAR in MDA-MB-436 cells did not render them insensitive to PARG inhibition.

Supplementary Table 1: Selectivity / Safety Panel Screening for Compound 4

Assay Target	Species	Concentration (μM)	% inhibition
Adenosine A_1	human	10	1
Adenosine A_{2A}	human	10	-1
Adrenergic α_{1A}	rat	10	-5
Adrenergic α_{1B}	rat	10	7
Adrenergic α_{2A}	human	10	10
Adrenergic β_1	human	10	-9
Adrenergic β_2	human	10	-9
Calcium Channel, L Type	rat	10	16
Cannabinoid CB_1	human	10	21
Dopamine D_1	human	10	6
Dopamine D_{2S}	human	10	-9
GABAA, Flunitrazepam, Central	rat	10	4
GABAA, Muscimol, Central	rat	10	3
Glutamate, NMDA,	rat	10	4
Histamine H_1	human	10	-6
Imidazoline I_2, Central	rat	10	-18
Muscarinic M_2	human	10	-1
Muscarinic M_3	human	10	3
Nicotinic Acetylcholine	human	10	3
Nicotinic Acetylcholine, a_1	human	10	-3
Opiate μ (OP3, MOP)	human	10	-6
Phorbol Ester	mouse	10	-11
Potassium Channel [K_{ATP}]	ham	10	5
Potassium Channel hERG	human	10	12
Prostanoid EP_4	human	10	11
Rolipram	rat	10	16
Serotonin (5-Hydroxytryptamine), 5-HT_{2B}	human	10	4
Sigma σ_1	human	10	15
Sodium Channel, site 2	rat	10	6
Transporter, Norepinephrine (NET)	human	10	20
Acetyl Cholinesterase	human	10	-1
Cyclooxygenase COX-2	human	10	-2
Phosphodiesterase PDE4	human	10	17

Supplementary Note 1. Previously reported classes of putative PARG inhibitors. These generally display only modest potency, lack of activity in whole-cell models, polypharmacoloy and/or PAINs motifs, and as such are considered undesirable chemical tools.

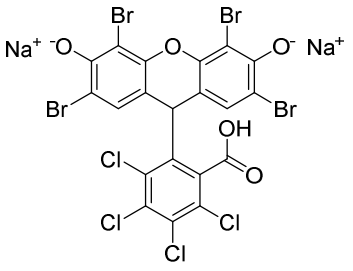

Phloxin B

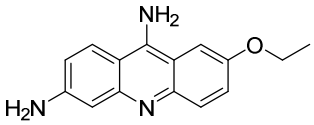

Ethacridine

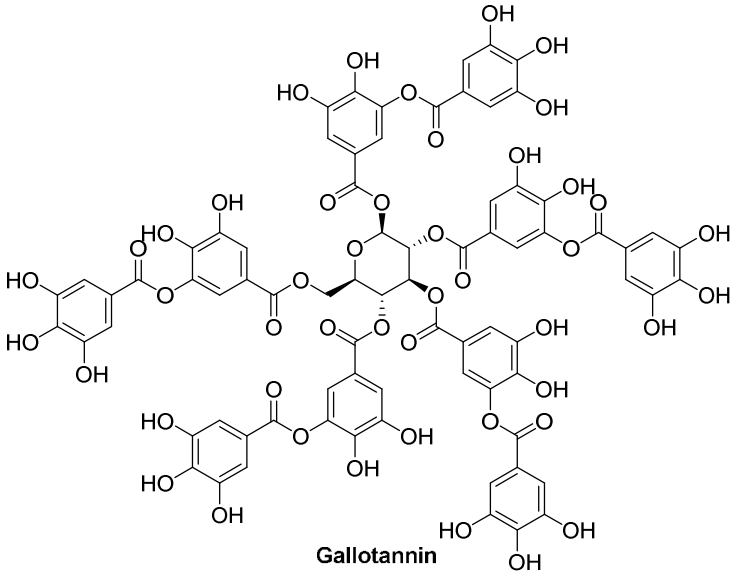

Gallotannin

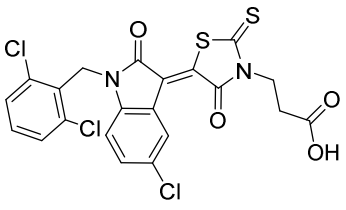

RPBI-3

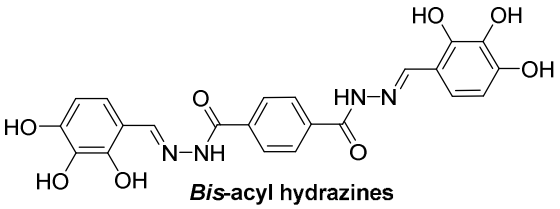

Bis-acyl hydrazines

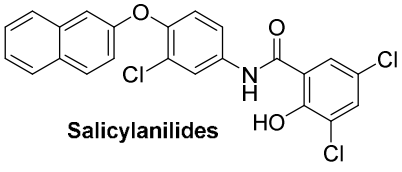

Salicylanilides

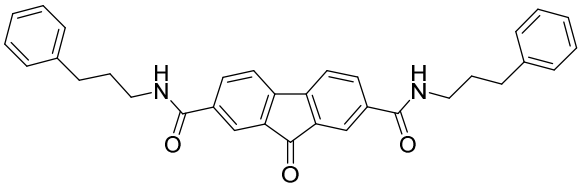

GPI-16552

Previously reported classes of putative PARG inhibitors (*contd.*).

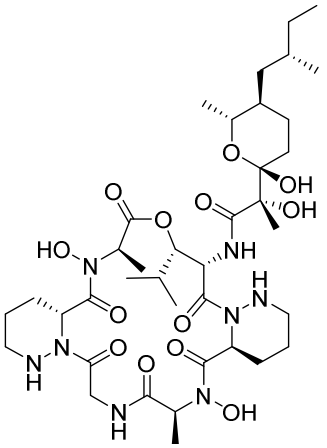

PD124966

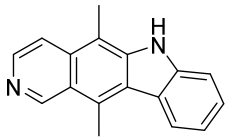

Ellipticine

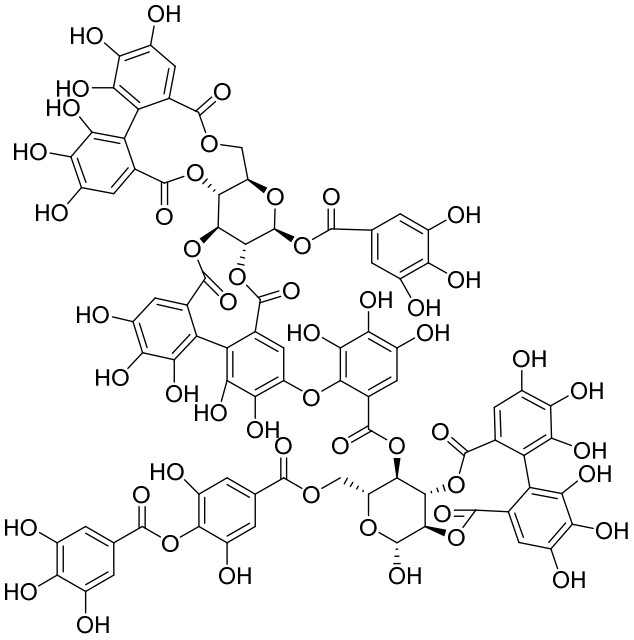

Nobotanin B

Supplementary Note 2: Synthetic Methods

Flash chromatography was performed using pre-packed silica gel cartridges (KP-Sil SNAP, Biotage, Hengoed UK or RediSep Rf, Isco). Thin layer chromatography was conducted with 5 × 10 cm plates coated with Merck Type 60 F_{254} silica gel to a thickness of 0.25 mm. All reagents obtained from commercial sources were used without further purification. Anhydrous solvents were obtained from the Sigma-Aldrich Chemical Company Ltd. or Fisher Chemicals Ltd., and used without further drying. HPLC grade solvents were obtained from Fisher Chemicals Ltd. All compounds were > 90% purity as determined by examination of both the LC-MS and ^{1}H NMR spectra unless otherwise indicated. Where Cl or Br were present, expected isotopic distribution patterns were observed.

^{1}H NMR

Proton (^{1}H) and carbon (^{13}C) NMR spectra were recorded on a 300 MHz Bruker spectrometer. Solutions were typically prepared in either deuterochloroform ($CDCl_3$) or deuterated dimethylsulfoxide (d^6-DMSO) with chemical shifts referenced to tetramethylsilane (TMS) or deuterated solvent as an internal standard. ^{1}H NMR data are reported indicating the chemical shift (δ), the integration (e.g. 1H), the multiplicity (s, singlet; d, doublet; t, triplet; q, quartet; m, multiplet; br, broad; dd, doublet of doublets etc.) and the coupling constant (J) in Hz (app implies apparent coupling on broadened signals). Deuterated solvents were obtained from the Sigma-Aldrich Chemical Company, Goss or Fluorochem.

Analytical LC-MS.

LC-MS analyses were performed on a Waters Acquity UPLC system fitted with BEH C18 1.7 μM columns (2.1 × 50 mm) and with UV diode array detection (210–400 nm). Positive and negative mass ion detection was performed using a Waters SQD detector. Analyses were performed with either buffered acidic or basic solvents and gradients as detailed below:

Low pH:

Solvent A – Water + 10mM ammonium formate + 0.1% formic acid
Solvent B – Acetonitrile + 5% water + 0.1% formic acid

High pH:

Solvent A – Water + 10mM ammonium hydrogen carbonate + 0.1% ammonia solution
Solvent B – Acetonitrile + 0.1% ammonia solution

Gradient:

Time (min)	Flow rate (mL min^{-1})	% Solvent A	% Solvent B
0	0.6	95	5
1.2	0.6	5	95
1.7	0.6	5	95
1.8	0.6	95	5

Preparative HPLC

Certain compounds were purified by preparative HPLC on a Waters FractionLynx MS autopurification system, with a Waters XBridge 5 μm C18, 100 mm × 19 mm i.d. column, running at a flow rate of 20 mL min^{-1} with UV diode array detection (210–400 nm) and mass-directed collection using both positive and negative mass ion detection. Purifications were performed using buffered acidic or basic solvent systems as appropriate. Compound retention times on the system were routinely assessed using a 30-50 μL test injection and a standard gradient, then purified using an appropriately chosen focussed gradient as detailed below, based upon observed retention time.

Low pH:

Solvent A – Water + 10 mM ammonium formate + 0.1% formic acid
Solvent B – Acetonitrile + 5% water +0.1% formic acid

High pH:

Solvent A – Water + 10mM ammonium formate + 0.1% ammonia solution
Solvent B – Acetonitrile + 5% water + 0.1% ammonia solution

Standard Gradient:

Time (min)	Flow rate (mL min^{-1})	% Solvent A	% Solvent B
0	20	90	10
0.3	20	90	10
8.5	20	2	98
12	20	2	98
12.5	0	2	98

Focussed Gradients:

		% Solvent B				
		Retention time on standard gradient (min.)				
Time (min)	Flow rate (mL min^{-1})	0 – 5.2	4.9 – 6.6	6.3 – 7.5	7.3 – 9.5	9.3 - 12
0	20	10	10	10	10	10
0.25	20	10	10	10	10	10
0.35	20	10	20	35	45	60
10	20	45	55	65	75	98
12	20	98	98	98	98	98
12.5	0	98	98	98	98	98

Preparation of 1-[(2,5-Dimethylpyrazol-3-yl)methyl]-N-(1-methylcyclopropyl)-3-[(2-methylthiazol-5-yl)methyl]-2,4-dioxo-quinazoline-6-sulfonamide (4) and 1-[(2,5-Dimethylpyrazol-3-yl)methyl]-N-methyl-N-(1-methylcyclopropyl)-3-[(2-methylthiazol-5-yl)methyl]-2,4-dioxo-quinazoline-6-sulfonamide (6).

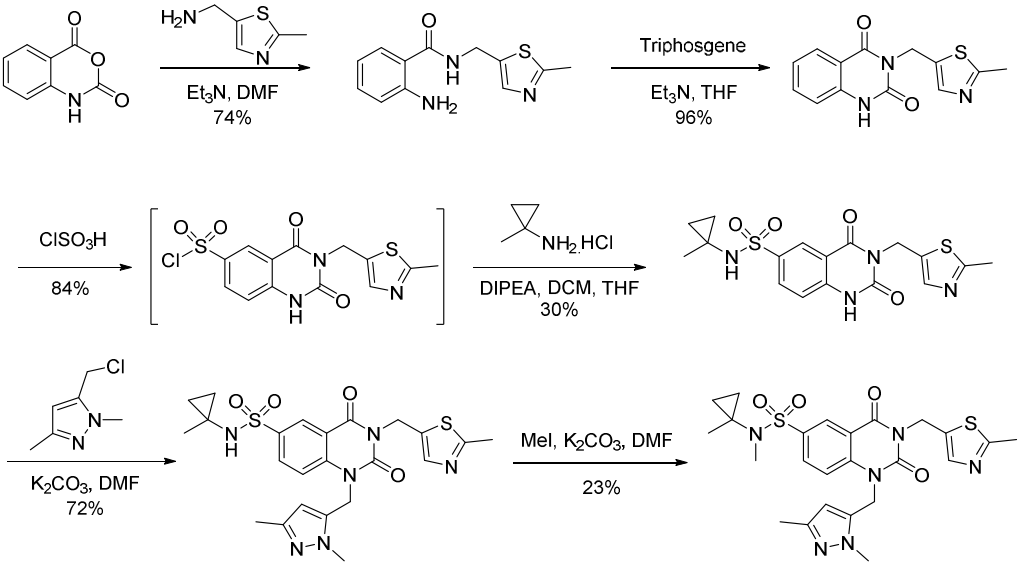

2-Amino-N-[(2-methylthiazol-5-yl)methyl]benzamide.

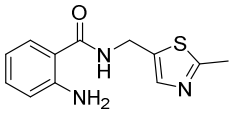

A solution of isatoic acid anhydride (2.55 g, 15.6 mmol) in DMF (35 mL) was cooled to 0 °C and treated with (2-methyl-1,3-thiazol-5-yl)methanamine (2.00 g, 15.6 mmol) and triethylamine (4.89 mL, 35.1 mmol). The resulting mixture was stirred at 50°C for 3 h and then cooled to RT. The solvent was removed in vacuo and the crude product was suspended in 10% MeOH/DCM (200 mL) and stirred for 30 min. The solid was then filtered and the filter cake washed with DCM (2 × 20 mL) and oven-dried to yield the title compound as a yellow powder (2.84 g, 11.5 mmol, 74% yield). ^{1}H NMR (300MHz, DMSO-d_6) δ = 8.85 (t, *J*=5.8 Hz, 1H), 7.48 (s, 1H), 7.46 (dd, *J*=1.5, 8.1 Hz, 1H), 7.14 (ddd, *J*=1.5, 7.0, 8.3 Hz, 1H), 6.69 (dd, *J*=1.0, 8.2 Hz, 1H), 6.55 - 6.42 (m, 3H), 4.52 (d, *J*=5.7 Hz, 2H), 2.65 - 2.56 (m, 3H). LCMS (high pH) found 246.1 $[M-H]^-$ T= 0.81 min.

3-[(2-Methylthiazol-5-yl)methyl]-1H-quinazoline-2,4-dione.

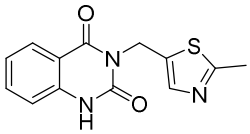

A solution of 2-amino-N-[(2-methylthiazol-5-yl)methyl]benzamide (2.84 g, 11.5 mmol) in THF (100 mL) was cooled to 0 °C and treated with triphosgene (1.70 g, 5.7 mmol). The resulting solution was stirred at RT for 16 h, forming a thick suspension. The reaction was quenched by the addition of sat. aq. K_2CO_3 (100 mL) and allowed to stir overnight at RT. The volatiles were removed in vacuo and the resulting suspension was diluted with EtOAc (400 mL) and water (200 mL). The aq. layer was re-extracted with EtOAc and the combined organic extracts were washed with brine, dried (hydrophobic frit) and concentrated. The crude material was suspended in DCM (200 mL), stirred for 30 min and filtered. The filter cake was washed with DCM (2 × 20 mL) and oven-dried to give the desired product as a white powder (3.01 g, 11.0 mmol, 96% yield). ^{1}H NMR (300MHz, DMSO-d_6) δ = 11.58 (br s, 1H), 7.94 (d, *J*=7.7 Hz, 1H), 7.66 (t, *J*=7.7 Hz, 1H), 7.59 (s, 1H), 7.26 - 7.14 (m, 2H), 5.19 (s, 2H), 2.59 - 2.53 (m, 3H). LCMS (high pH) found 274.1 $[M+H]^+$ T= 0.83 min.

3-[(2-Methylthiazol-5-yl)methyl]-2,4-dioxo-1H-quinazoline-6-sulfonyl chloride.

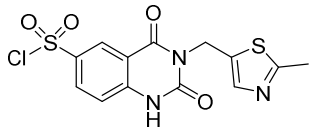

A solution of 3-[(2-methylthiazol-5-yl)methyl]-1H-quinazoline-2,4-dione (930 mg, 3.4 mmol) in chlorosulfonic acid (2.0 mL) was heated to 60°C with stirring for 3 h. The mixture was then allowed to cool and added cautiously drop wise to iced water (~30 mL). The precipitated solid was filtered off and the filtrate extracted with CH_2Cl_2 and EtOAc. The solid and organic liquors were combined and evaporated to dryness to give the title compound as a brown solid (1.06 g). This was used immediately in the next step without purification.

N-(1-Methylcyclopropyl)-3-[(2-methylthiazol-5-yl)methyl]-2,4-dioxo-1H-quinazoline-6-sulfonamide.

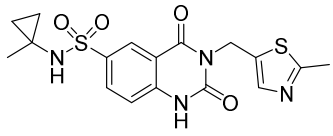

A solution of 1-methylcyclopropanamine hydrochloride (0.92 g, 8.6 mmol) and N,N-diisopropylethylamine (2.83 mL, 17.1 mmol) in a mixture of DCM (30 mL) and THF (30 mL) was treated portionwise with 3-[(2-methylthiazol-5-yl)methyl]-1H-quinazoline-2,4-dione-6-sulfonyl chloride (1.06 g, 2.9 mmol) and the mixture stirred at RT for 3 h. The solvent was then removed under reduced pressure, and the residue was flash chromatographed over silica (CH_2Cl_2, diethyl ether/MeOH gradient elution to give the title compound as a white powder (350 mg, 0.86 mmol, 25% yield over two steps). ^{1}H NMR (300MHz, DMSO-d_6) δ = 11.97 (s, 1H), 8.32 (d, *J*=2.1 Hz, 1H), 8.14

(s, 1H), 8.01 (dd, *J*=2.2, 8.6 Hz, 1H), 7.61 (s, 1H), 7.33 (d, *J*=8.6 Hz, 1H), 5.19 (s, 2H), 2.58 - 2.56 (m, 3H), 1.06 (s, 3H), 0.62 - 0.54 (m, 2H), 0.43 - 0.34 (m, 2H). LCMS (high pH) found 407.3 $[M+H]^+$ T= 0.86 min.

1-[(2,5-Dimethylpyrazol-3-yl)methyl]-N-(1-methylcyclopropyl)-3-[(2-methylthiazol-5-yl)methyl]-2,4-dioxo-quinazoline-6-sulfonamide 4.

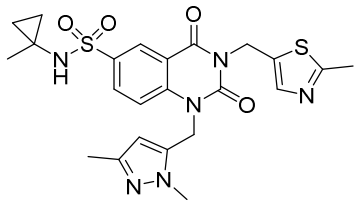

A mixture of N-(1-methylcyclopropyl)-3-[(2-methylthiazol-5-yl)methyl]-1H-quinazoline-2,4-dione-6-sulfonamide (350 mg, 0.86 mmol), K_2CO_3 (179 mg, 1.3 mmol) and 5-(chloromethyl)-1,3-dimethyl-1H-pyrazole (162 mg, 1.1 mmol) in DMF (10 mL) was heated in the microwave at 80°C for 30 min. The reaction mixture was then diluted with water (100 mL) and extracted with EtOAc (2 x 100 mL). The combined organic extracts were washed with water, dried (hydrophobic frit), concentrated and the residue was flash chromatographed over silica (CH_2Cl_2/diethyl ether/MeOH gradient elution). The product-containing fractions were combined and concentrated, then triturated with diethyl ether to give the title compound as a white powder (320 mg, 0.62 mmol, 72% yield). ^{1}H NMR (300MHz, DMSO-d_6) δ = 8.44 (d, *J*=2.3 Hz, 1H), 8.23 (s, 1H), 8.03 (dd, *J*=2.3, 8.9 Hz, 1H), 7.64 (s, 1H), 7.56 (d, *J*=8.9 Hz, 1H), 5.76 (s, 1H), 5.38 (s, 2H), 5.26 (s, 2H), 3.82 (s, 3H), 2.58 (s, 3H), 1.99 (s, 3H), 1.07 (s, 3H), 0.63 - 0.55 (m, 2H), 0.42 - 0.36 (m, 2H). ^{13}C NMR (75MHz, CHLOROFORM-d) δ = 159.80, 150.06, 147.82, 142.72, 141.96, 137.85, 136.46, 133.54, 131.27, 128.79, 125.23, 115.75, 115.07, 105.35, 39.63, 37.38, 36.67, 31.81, 24.61, 18.97, 14.07 (2C), 13.32. LCMS (high pH) found 515.7 $[M+H]^+$ T= 0.98 min. HRMS *m/z*: $[M+H]^+$ Calcd for $C_{23}H_{27}N_6O_4S_2$ 515.1530; Found 515.1516.

1-[(2,5-Dimethylpyrazol-3-yl)methyl]-N-methyl-N-(1-methylcyclopropyl)-3-[(2-methylthiazol-5-yl)methyl]-2,4-dioxo-quinazoline-6-sulfonamide 6.

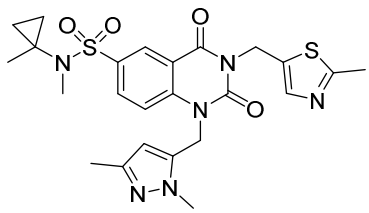

A mixture of 3-((1-methyl-1H-pyrazol-4-yl)methyl)-N-(1-methylcyclopropyl)-quinazoline-2,4-dione-6-sulfonamide (120 mg, 0.31 mmol), K_2CO_3 (16 mg, 0.12 mmol) and iodomethane (6.7 uL, 0.11 mmol) in DMF (2 mL) was stirred at RT for 21 h. A further 0.5 eq. MeI was added and the mixture was stirred at RT for a further 2 h, then diluted with water (2 mL) and DCM (5 mL). The biphasic

mixture was stirred vigorously for 10 min and passed through a hydrophobic frit. The aq. layer was re-extracted with DCM (5 mL), and the combined organic extracts were concentrated and purified by prep. HPLC (high pH) to give the title compound as a white powder (12 mg, 0.023 mmol, 23% yield). ^{1}H NMR (300MHz, DMSO-d_6) δ = 8.35 (d, *J*=2.3 Hz, 1H), 8.06 (dd, *J*=2.4, 8.9 Hz, 1H), 7.63 (s, 1H), 7.55 (d, *J*=9.0 Hz, 1H), 5.78 (s, 1H), 5.38 (s, 2H), 5.26 (s, 2H), 3.82 (s, 3H), 2.81 (s, 3H), 2.59 - 2.56 (m, 3H), 2.00 (s, 3H), 1.06 (s, 3H), 0.93 - 0.87 (m, 2H), 0.65 - 0.59 (m, 2H). ^{13}C NMR (75MHz, CHLOROFORM-d) δ = 167.50, 159.74, 150.05, 147.88, 143.41, 141.90, 136.35, 136.34, 133.81, 131.07, 129.01, 115.76, 114.95, 105.38, 39.57, 37.98, 37.42, 36.63, 34.35, 20.24, 19.13, 16.19 (2C), 13.31. LCMS (high pH) found 529.2 $[M+H]^+$ T= 1.06 min. HRMS *m/z*: $[M+H]^+$ Calcd for $C_{24}H_{29}N_6O_4S_2$, 529.1692; found, 529.1700.

Preparation of 1-((2,4-Dimethylthiazol-5-yl)methyl)-N-(1-methylcyclopropyl)-2-oxo-3-(1,2,4-thiadiazol-5-yl)-2,3-dihydro-1H-benzo[d]imidazole-5-sulfonamide (5) and 1-[(2,4-dimethylthiazol-5-yl)methyl]-N-methyl-N-(1-methylcyclopropyl)-2-oxo-3-(1,2,4-thiadiazol-5-yl)benzimidazole-5-sulfonamide (7).

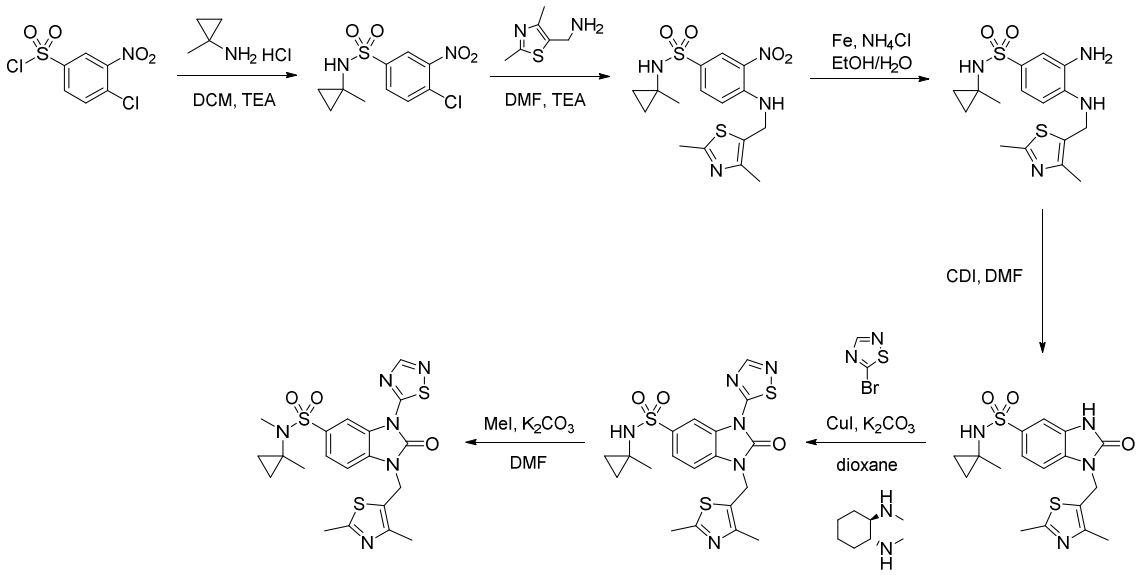

4-Chloro-N-(1-methylcyclopropyl)-3-nitro-benzenesulfonamide.

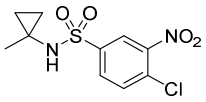

Triethylamine (1.63 mL, 11.72 mmol) was added in a dropwise manner to a stirred solution of 4-chloro-3-nitrobenzenesulfonyl chloride (1.0 g, 3.91 mmol) and 1-methylcyclopropanamine hydrochloride (0.46 g, 4.3 mmol) in DCM (20 mL), and the resulting mixture was stirred for 2 h. The mixture was then quenched with saturated potassium carbonate solution (20 mL). The DCM layer was collected and evaporated under reduced pressure to give a residue, which was purified by automated column chromatography over silica gel (0−100% EtOAc in iso-hexane) to give the desired product as a brown solid (1.07 g, 3.68 mmol, 94%). ^{1}H NMR (300 MHz, $CDCl_3$) δ = 8.39 (d, *J* = 2.2 Hz, 1H), 8.03 (dd, *J* = 2.2, 8.5 Hz, 1H), 7.72 (d, *J* = 8.5 Hz, 1H), 5.28 (s, 1H), 1.29 (s, 3H), 0.82–0.72 (m, 2H), 0.65–0.49 (m, 2H). LCMS (high pH) found 291.2 $[M+H]^+$ T = 1.04 min.

4-[(2,4-Dimethylthiazol-5-yl)methylamino]-N-(1-methylcyclopropyl)-3-nitro-benzenesulfonamide.

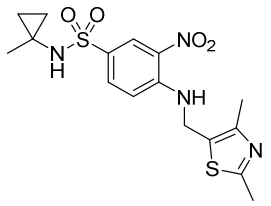

(Dimethyl-1,3-thiazol-5-yl)methanamine (7.52 mL, 7.03 mmol) was added in a dropwise manner to a stirred solution of 4-chloro-N-(1-methylcyclopropyl)-3-nitro-benzenesulfonamide (2.04 g, 7.03 mmol) and triethylamine (1.47 mL, 10.55 mmol) in DMF (30 mL), and the resulting mixture was heated at 130 °C for 6 h. The reaction was cooled to room temperature and quenched by the addition of water (20 mL). The DCM layer was collected and evaporated to dryness to give a residue, which was purified by column chromatography over silica gel (0–10% MeOH in DCM) to give the desired product as a yellow solid (2.39 g, 6.04 mmol, 86%). This material was progressed into the subsequent step without full characterization. LCMS (high pH) found 397.5 $[M+H]^+$ T = 1.07 min.

3-Amino-4-[(2,4-dimethylthiazol-5-yl)methylamino]-N-(1 methylcyclopropyl)benzenesulfonamide.

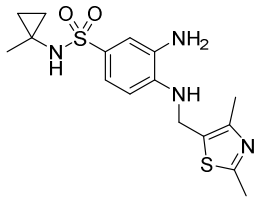

To a magnetically stirred suspension of iron (1.69 g, 30.23 mmol) in ethanol (25 mL) was added 4-[(2,4-dimethylthiazol-5-yl)methylamino]-N-(1-methylcyclopropyl)-3-nitro-benzenesulfonamide (2.4 g, 6.05 mmol), ammonium chloride (1.62 g, 30.23 mmol) and water (25 mL), and the resulting mixture was stirred for 2 h at 80 °C. The mixture was filtered hot through celite and the filter cake washed with hot ethanol. The combined filtrate was concentrated under reduced pressure to give a slurry, which was partitioned between water (80 mL) and DCM (80 mL). The organic layer was separated and the aqueous layer extracted with DCM (2 × 30 mL). The combined organics were dried (Na_2SO_4) and concentrated under vacuum to give a residue, which was purified by column chromatography over silica gel (0–10% MeOH in DCM) to give the desired product as an off-white solid (1.99 g, 5.43 mmol, 90%). ^{1}H NMR (300MHz, $CDCl_3$): δ = 7.39 (dd, *J* = 2.0, 8.3 Hz, 1H), 7.24 (d, *J* = 2.1 Hz, 1H), 6.69 (d, *J* = 8.4 Hz, 1H), 4.74 (s, 1H), 4.43 (d, *J* = 5.2 Hz, 2H), 4.09 (br. s., 1H), 3.41 (br. s., 2H), 2.66 (s, 3H), 2.42 (s, 3H), 1.22 (s, 3H), 0.87–0.77 (m, 2H), 0.51–0.42 (m, 2H). LCMS (low pH) found 367.6 $[M+H]^+$ T = 0.88 min.

1-[(2,4-Dimethylthiazol-5-yl)methyl]-N-(1-methylcyclopropyl)-2-oxo-3H-benzimidazole-5-sulfonamide.

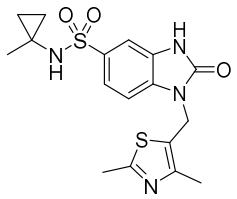

A magnetically stirred solution of 3-amino-4-[(2,4-dimethylthiazol-5-yl)methylamino]-N-(1-methylcyclopropyl)benzenesulfonamide (1.99 g, 5.43 mmol) and 1,1'-carbonyldiimidazole (1.76 g, 10.86 mmol) in acetonitrile (20 mL) was heated at reflux for 2 h. The mixture was cooled to room temperature and evaporated to dryness to give a residue, which was partitioned between DCM (30 mL) and water (30 mL). The DCM layer was concentrated under reduced pressure to give a residue, which was purified by column chromatography of silica gel (0–10% MeOH in DCM) to give the desired product as an off-white solid (1.74 g, 4.05 mmol, 75%). ^{1}H NMR (300MHz, DMSO-d_6): δ = 11.36 (s, 1H), 7.90 (s, 1H), 7.49 (dd, *J* = 1.8, 8.3 Hz, 1H), 7.36 (d, *J* = 1.8 Hz, 1H), 7.26 (d, *J* = 8.3 Hz, 1H), 5.16 (s, 2H), 2.50 (s, 3H), 2.43 (s, 3H), 1.02 (s, 3H), 0.66–0.50 (m, 2H), 0.40–0.29 (m, 2H). LCMS (high pH) found 393.5 $[M+H]^+$ T = 0.88 min.

1-((2,4-Dimethylthiazol-5-yl)methyl)-N-(1-methylcyclopropyl)-2-oxo-3-(1,2,4-thiadiazol-5-yl)-2,3-dihydro-1H-benzo[d]imidazole-5-sulfonamide 5.

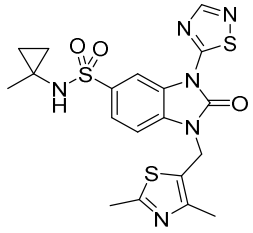

A magnetically stirred mixture of 1-[(2,4-dimethylthiazol-5-yl)methyl]-N-(1-methylcyclopropyl)-2-oxo-3H-benzimidazole-5-sulfonamide (300 mg, 0.76 mmol, 5-bromo-1,2,4-thiadiazole (189 mg, 1.15 mmol), copper iodide (29 mg, 0.15 mmol) and potassium carbonate (422 mg, 3.06 mmol) in 1,4-dioxane (8 mL) was degassed with nitrogen for 5 min. *trans*-N,N'-Dimethylcyclohexane-1,2-diamine (48.21 uL, 0.31 mmol) was then added to the reaction, and the resulting mixture was heated at reflux under nitrogen for 4 h. The mixture was cooled to room temperature and partitioned between DCM (10 mL) and saturated potassium carbonate solution (10 mL). DCM layer was collected and

concentrated under reduced pressure to give a residue, which was purified by preparatory HPLC to give the desired product as a pale yellow powder (92 mg, 0.19 mmol, 25%) ^{1}H NMR (300 MHz, $CDCl_3$): δ = 8.95 (s, 1H), 8.47 (s, 1H), 7.84 (br d, *J* = 8.3 Hz, 1H), 7.18–7.10 (m, 1H), 5.29–5.09 (m, 2H), 4.89 (s, 1H), 2.52 (br d, *J* = 10.5 Hz, 6H), 1.23–1.13 (m, 3H), 0.74 (br s, 2H), 0.44 (s, 2H). ^{13}C NMR (75MHz, DMSO-d_6): δ = 172.18, 164.06, 159.29, 151.59, 150.30, 137.34, 131.93, 124.83, 124.21, 123.59, 111.73, 109.60, 36.96, 30.87, 23.96, 18.68, 14.98, 12.98. LCMS (high pH) found 477.5 $[M+H]^+$ T= 1.10 min. HRMS (ESI): *m/z* 477.0816 for $[M+H]^+$; Calcd for $C_{19}H_{21}N_6O_3S_3$ 477.0837

1-[(2,4-dimethylthiazol-5-yl)methyl]-N-methyl-N-(1-methylcyclopropyl)-2-oxo-3-(1,2,4-thiadiazol-5-yl)benzimidazole-5-sulfonamide 7.

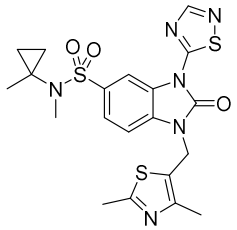

To a magnetically stirred solution of 1-[(2,4-dimethylthiazol-5-yl)methyl]-N-(1-methylcyclopropyl)-2-oxo-3-(1,2,4-thiadiazol-5-yl)benzimidazole-5-sulfonamide (50 mg, 0.10 mmol) and potassium carbonate (20 mg, 0.15 mmol) in DMF (1 mL) at 20 °C under nitrogen was added iodomethane (9.1 uL, 0.15 mmol), and the resulting mixture was agitated at room temperature for 16 h. The mixture was partitioned between DCM (10 mL) and saturated potassium bicarbonate (10 mL). The organic phase was collected and distilled to dryness to give a residue, which was purified by prep. HPLC (high pH) to give the desired product as a white solid (20 mg, 0.04 mmol, 39%). ^{1}H NMR (300MHz, DMSO-d_6): δ = 8.84 (s, 1H), 8.74 (d, *J* = 1.8 Hz, 1H), 7.83 (dd, *J* = 1.8, 8.4 Hz, 1H), 7.68 (d, *J* = 8.4 Hz, 1H), 5.40 (s, 2H), 2.83 (s, 3H), 2.50 (s, 6H), 1.08 (s, 3H), 0.98–0.89 (m, 2H), 0.68–0.59 (m, 2H). ^{13}C NMR (75 MHz, DMSO-d_6): δ = 172.22, 164.10, 159.36, 151.56, 150.36, 134.44, 132.34, 124.94, 124.15, 112.10, 109.80, 37.49, 36.97, 34.05, 19.38, 18.69, 15.63, 14.98. LCMS (high pH) found 491.1 $[M+H]^+$ T= 1.21 min. HRMS (ESI): *m/z* 491.0972 for $[M+H]^+$; Calcd for $C_{20}H_{23}N_6O_3S_3$ 491.0993.

1H NMR spectrum for Compound **4**:

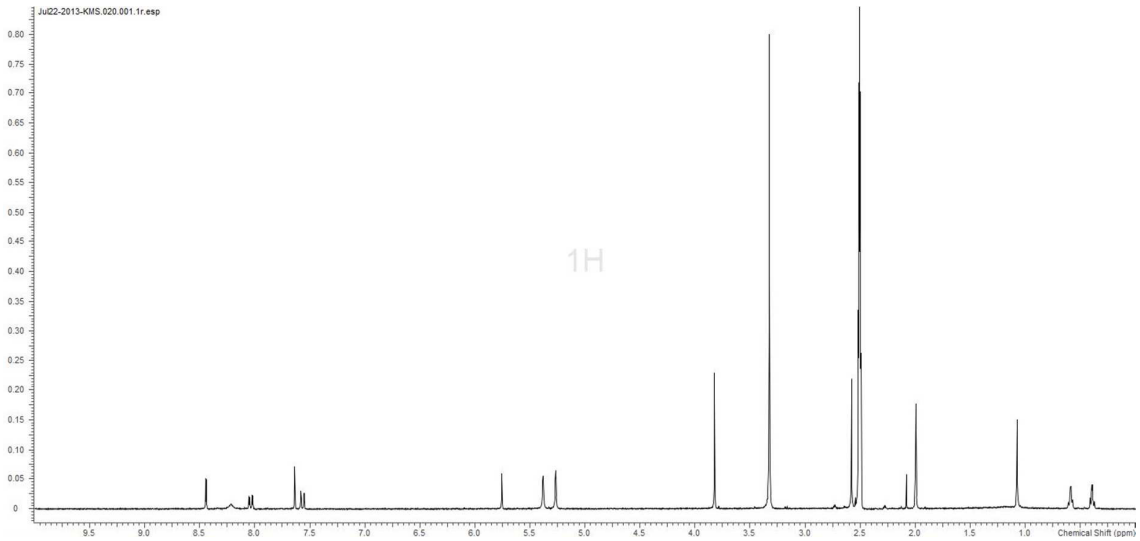

1H NMR spectrum for Compound **6**:

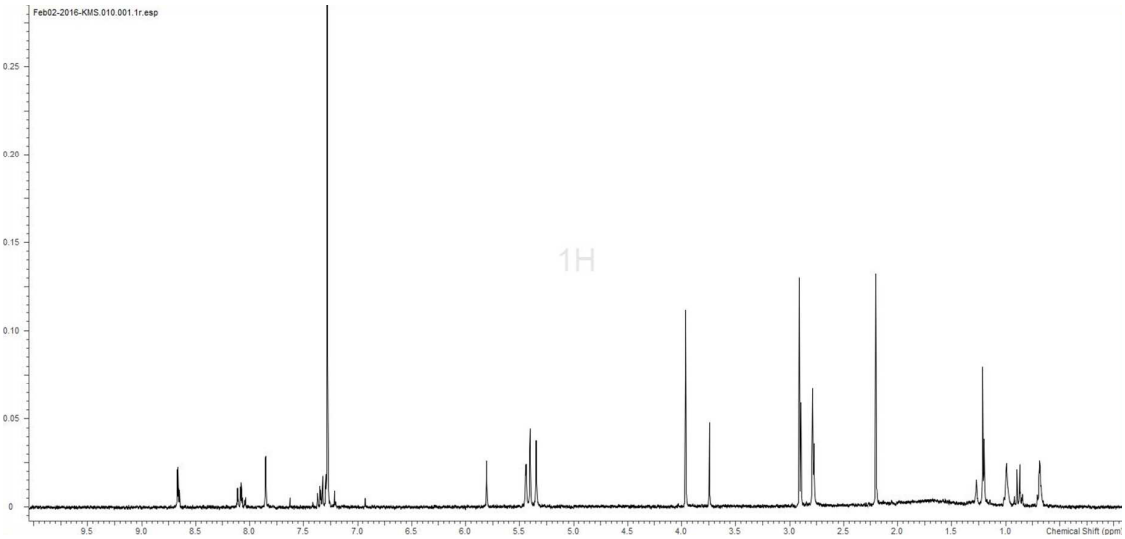

1H NMR spectrum for Compound **5**:

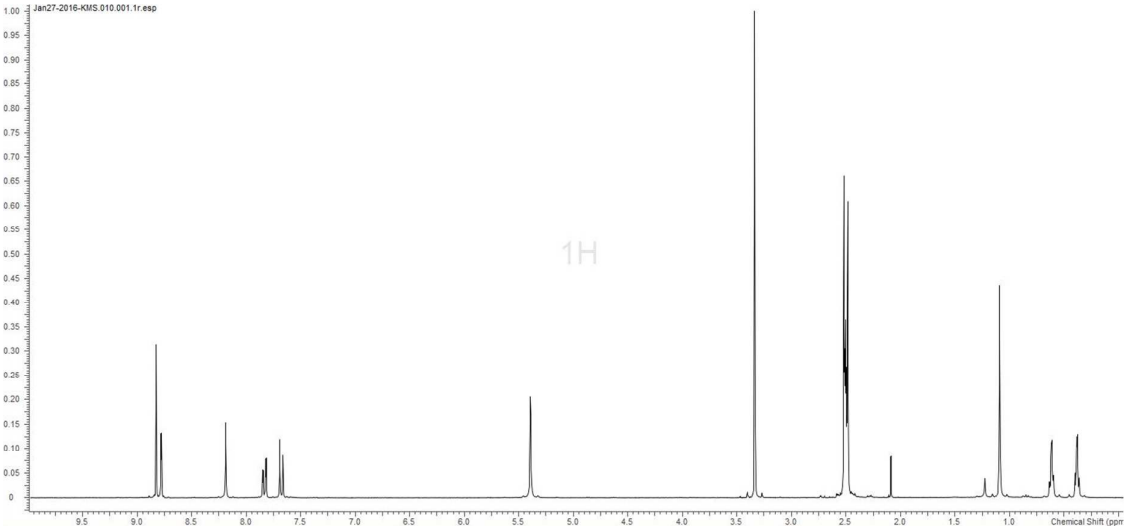

1H NMR spectrum for Compound **7**:

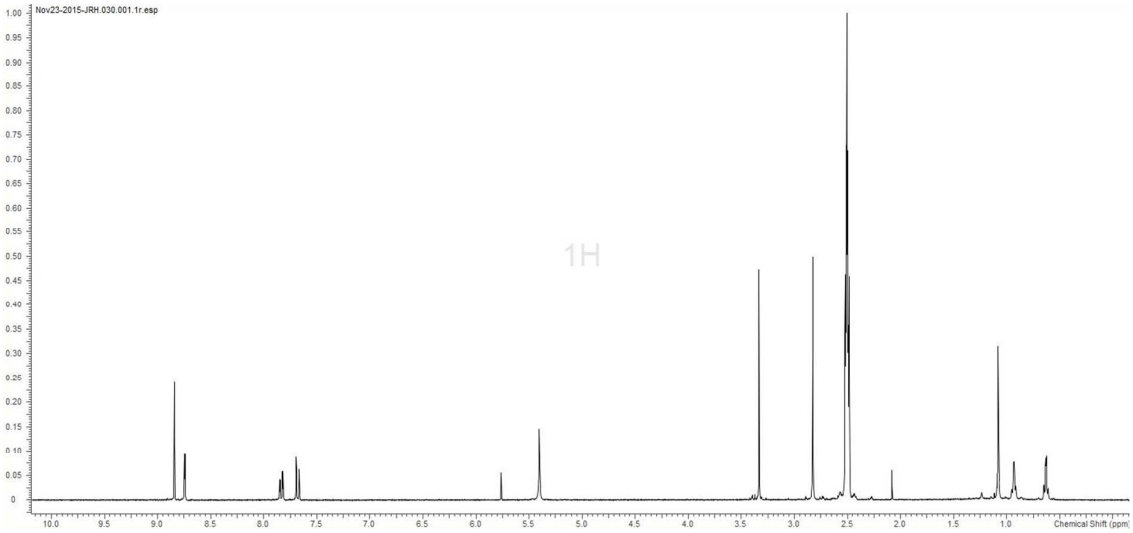

PARG co-crystal structure determination and refinement details

Protein Expression, Purification and Crystallisation

Human PARG catalytic domain surface entropy mutant (PARG(448-976 [K617A, Q618A, K619A, E688A, K689A, K690A])) was expressed, purified and crystallized as described[1] with minor modifications as follows.

Expression in *E. coli* BL21 GOLD was carried out at 15 L scale in shake flasks. Expression was induced, and cells harvested and lysed as described.[1] Buffers used for purification were as described.[1] 6His-TEV-PARG(448-976 [K617A, Q618A, K619A, E688A, K689A, K690A]) was purified from the clarified lysate by immobilised metal affinity chromatography (IMAC) using a 5 mL His-TRAP HP column (GE Healthcare). Pooled fractions enriched for 6His-TEV-PARG(448-976 [K617A, Q618A, K619A, E688A, K689A, K690A]) were incubated with 6His-tagged TEV protease whilst being dialysed for 24 hours at 4 ºC. Cleaved PARG was separated from uncleaved material, 6His tag and TEV protease by subtractive IMAC using a 5 mL His-TRAP HP column (GE Healthcare). The unbound material was concentrated using a 10 kDa MWCO Vivaspin® 20 (Sartorius) concentrator before loading on a 125 mL Superdex200 sizing column (GE Healthcare). IMAC and size exclusion chromatography were automated and injection, wash and elution steps performed on an ÄKTA™ Unicorn FPLC system (GE Healthcare). Pooled fractions containing GS-PARG(448-976 [K617A, Q618A, K619A, E688A, K689A, K690A]) were concentrated to 7.5 mg/mL. Typically, <0.15 mg purified GS-PARG(448-976 [K617A, Q618A, K619A, E688A, K689A, K690A]) was obtained per litre culture.

Reproducible crystallisation was ensured by seeding as follows. Crystals were grown at 293 K by sitting-drop vapour diffusion in an Intelli-plate® (Hampton Research) by mixing 750 nL purified protein at 7.5 mg/mL in 50 mM HEPES, pH 7.0, 150 mM NaCl, 2 mM DTT with 250 nL of seed stock and 1000 nL of a precipitant consisting of 18-23 % (w/v) PEG-3350, 0.2 M ammonium sulphate, 0.1 M PCTP pH 7.5. Seed stock was prepared using a Seed Bead™ (Hampton Research) from a co-crystal of GS-PARG(448-976 [K617A, Q618A, K619A, E688A, K689A, K690A]) with

ADP-ribose, with co-crystallisation mother liquor (19 % (w/v) PEG-3350, 0.2 M ammonium sulphate, 0.1 M PCTP pH 7.5) as the stabilising solution. The final volume of the seed stock was 100 μL. Crystals appeared over 48 hours and continued to grow for a further week.

Formation of Ligand Complexes by Crystal Soaking

Complex structures were obtained by incubating crystals of PARG(448-976 [K617A, Q618A, K619A, E688A, K689A, K690A]) for 3½ days in a soak buffer (25 % (w/v) PEG-3350, 0.2 M ammonium sulphate, 0.1 M PCTP pH 8.5, 10 % (v/v) glycerol) containing the compound of interest (at a final concentration of 1 mM) and 10 % (v/v) DMSO. Crystals were then flash cooled in a gaseous nitrogen stream at 100 K prior to data collection.

Diffraction Data Collection, Structure Solution and Refinement

Diffraction data were collected at 100 K at the DIAMOND synchrotron radiation source as specified in Table S2. Data integration, scaling and reduction was carried out using XDS[2] and programs from the CCP4 suite[3, 4] as implemented within the automated data processing pipelines pipedream[5] xia2[6], EDNA[7] and autoPROC.[8] Structure solution by molecular replacement (using PDB ID 4A0D), initial refinement and ligand fitting were carried out using Phaser,[9] Buster[10] and Rhofit[11] as implemented within the automated pipeline, pipedream.[5] Compound coordinates and restraint dictionaries were generated from the corresponding SMILES string using Grade.[12] The protein-compound complex model was refined using Refmac[13-15] and/or Buster[10] with intermediate rounds of model building in Coot.[16] The stereochemical quality of the final models was checked using the MolProbity[17] structure validation tools available through Coot[16] for the protein component, and against the CSD[18] using Mogul[19] for the small molecule component. Simulated-annealing OMIT maps were calculated using *phenix.refine*.[20] The final structures have been deposited in the Protein Data Bank together with structure factors and detailed experimental conditions (see Table S2 for crystallographic statistics and PDB accession codes).

Supplementary Table 2. Crystallographic statistics for the structure of the human PARG catalytic domain in complex with PDD17262

Compound	**3**
PDB ID	5LHB
Soak conc'n (mM)	1
Soak time (days)	3½
Beam-line	DIAMOND, I02
Wavelength (Å)	0.979
Detector type	Pilatus 6M
Data collection date	11/07/2013
Space group	$P2_12_12_1$
Cell constants a; b; c (Å)	67.01; 89.73; 95.44
Resolution range (Å) [1]	33.51-2.23 (2.37-2.23)
Completeness overall (%)[1]	99.8 (99.7)
Reflections, unique	28669
Multiplicity[1]	5.7 (5.5)
Mean(I)/sd(I)[1]	8.6 (3)
*R*merge $_{overall}$ [2]	0.109 (0.614)
*R*value $_{overall}$ (%) [3]	16.47
*R*value $_{free}$ (%)[1]	21.15
Non hydrogen protein atoms	4090
Non hydrogen ligand atoms	31
Solvent molecules	300
R.m.s. deviations from ideal values	
Bond lengths (Å)	0.010
Bond angles (°)	0.99
Average *B* values (Å^2)	
Protein main chain atoms	41.4
Protein all atoms	43.7
Ligand	36.0
Solvent	54.7
Φ, Ψ angle distribution for residues [4]	
In most favoured regions (%)	90.5
In additional allowed regions (%)	8.8
In generously regions (%)	0.4
In disallowed regions (%)	0.2

Notes for Supplementary Table 2:

1 Values in parentheses refer to the outer resolution shell

2 $R_{\text{merge}} = \mathrm{S}_{hkl} [(\Sigma_i |I_i - \langle I \rangle|)/ \Sigma_i I_i]$

3 $R_{\text{value}} = \mathrm{S}_{hkl} ||F_{\text{obs}}| - |F_{\text{calc}}|| / \mathrm{S}_{hkl} |F_{\text{obs}}|$

R_{free} is the cross-validation R factor computed for the test set of 5% of unique reflections

4 Ramachandran statistics as defined by PROCHECK.[21]

Supplementary Note 3: – Supplementary biological methods

Western blotting

Cells were plated at between 2–3 × 10^6 cells in 10 mL media in a 10 cm dish. After 16–24 h at 37°C, the plates were removed onto ice and cells washed with 10 mL ice-cold PBS. Cells were then lysed in RIPA buffer (Sigma #R0278) with HALT protease and phosphatase inhibitor (Life Technologies Ltd), Pepstatin (10 µg/mL) and 5 mM EDTA on ice. Extracts were collected by scraping and incubated for a further 20 min on ice and centrifuged at 14,000*g* for 10 min at 4°C prior to protein quantitation using Direct Detect (Merck Millipore). Total protein (40 µg $well^{-1}$) and purified protein control (100 ng full length human PARG, 10 U PARP-HSA – Trevigen) was loaded on an all KD gel (Bio-Rad) and transferred to PVDF using Turbo blotter (Bio-Rad). After blocking with 5% non-fat milk powder in PBS the membranes were incubated with primary antibodies (PARP 46D11, Cell Signalling #9532; Actin AC40, Sigma A4700; PARG, Abcam Ab125446; PAR 10H, Merck-Millipore AM80) in PBS/0.1% Tween20/1% non-fat milk powder overnight at 4°C. Membranes were washed three times with wash buffer (PBS/0.1% Tween20) and incubated with secondary antibody in PBS/5% non-fat milk powder for 1 h. Membranes were then washed with wash buffer and incubated with SuperSignal West Pico chemiluminescent substrate (Life Technologies Ltd) according to manufacturer's instructions. Images were captured using G-Box (Syngene).

References and notes.

1. Tucker, J. A., Bennett, N., Brassington, C., Durant, S. T., Hassall, G., Holdgate, G., McAlister, M., Nissink, J. W., Truman, C., and Watson, M. (2012) Structures of the human poly (ADP-ribose) glycohydrolase catalytic domain confirm catalytic mechanism and explain inhibition by ADP-HPD derivatives, *PLoS One 7*, e50889.
2. Kabsch, W. (2010) XDS, *Acta Crystallogr. D Biol. Crystallogr. 66*, 125–132.
3. Evans, P. (2006) Scaling and assessment of data quality, *Acta Crystallogr. D Biol. Crystallogr. 62*, 72–82.
4. Winn, M. D., Ballard, C. C., Cowtan, K. D., Dodson, E. J., Emsley, P., Evans, P. R., Keegan, R. M., Krissinel, E. B., Leslie, A. G., McCoy, A., McNicholas, S. J., Murshudov, G. N., Pannu, N. S., Potterton, E. A., Powell, H. R., Read, R. J., Vagin, A., and Wilson, K. S. (2011) Overview of the CCP4 suite and current developments, *Acta Crystallogr. D Biol. Crystallogr. 67*, 235–242.
5. Sharff, A., Keller, P., Vonrhein, C., Smart, O., Womack, T., Flensburg, C., Paciorek, W., and Bricogne, G. (2011) Pipedream, version 0.1.5., *Global Phasing Ltd, Cambridge, United Kingdom.*
6. Winter, G. (2010) xia2: an expert system for macromolecular crystallography data reduction, *J. Appl. Crystallogr. 43*, 186–190.
7. Incardona, M. F., Bourenkov, G. P., Levik, K., Pieritz, R. A., Popov, A. N., and Svensson, O. (2009) EDNA: a framework for plugin-based applications applied to X-ray experiment online data analysis, *J. Synchrotron Radiat. 16*, 872–879.
8. Vonrhein, C., Flensburg, C., Keller, P., Sharff, A., Smart, O., Paciorek, W., Womack, T., and Bricogne, G. (2011) Data processing and analysis with the autoPROC toolbox, *Acta Crystallogr. D Biol. Crystallogr. 67*, 293–302.
9. McCoy, A. J., Grosse-Kunstleve, R. W., Adams, P. D., Winn, M. D., Storoni, L. C., and Read, R. J. (2007) Phaser crystallographic software, *J. Appl. Crystallogr. 40*, 658–674.
10. Bricogne, G., Blanc, E., Brandl, M., Flensburg, C., Keller, P., Paciorek, W., Roversi, P., Sharff, A., Smart, O., Vonrhein, C., and Womack, T. (2011) BUSTER version 111.5., *Global Phasing Ltd, Cambridge, United Kingdom.*
11. Womack, T. O., Smart, O., Sharff, A., Flensburg, C., Keller, P., Paciorek, W., Vonrhein, C., and Bricogne, G. (2011) Rhofit, version 1.2.3. , *Global Phasing Ltd, Cambridge, United Kingdom.*
12. Smart, O., Womack, T., Sharff, A., Flensburg, C., Keller, P., Paciorek, W., Vonrhein, C., and Bricogne, G. (2011) Grade, version 1.2.3., *Global Phasing Ltd., Cambridge, United Kingdom.*
13. Murshudov, G. N., Skubak, P., Lebedev, A. A., Pannu, N. S., Steiner, R. A., Nicholls, R. A., Winn, M. D., Long, F., and Vagin, A. A. (2011) REFMAC5 for the refinement of macromolecular crystal structures, *Acta Crystallogr. D Biol. Crystallogr. 67*, 355–367.
14. Murshudov, G. N., Vagin, A. A., and Dodson, E. J. (1997) Refinement of macromolecular structures by the maximum-likelihood method, *Acta Crystallogr. D Biol. Crystallogr. 53*, 240–255.
15. Winn, M. D., Murshudov, G. N., and Papiz, M. Z. (2003) Macromolecular TLS refinement in REFMAC at moderate resolutions, *Methods Enzymol. 374*, 300–321.
16. Emsley, P., Lohkamp, B., Scott, W. G., and Cowtan, K. (2010) Features and development of Coot, *Acta Crystallogr. D Biol. Crystallogr. 66*, 486–501.
17. Chen, V. B., Arendall, W. B., 3rd, Headd, J. J., Keedy, D. A., Immormino, R. M., Kapral, G. J., Murray, L. W., Richardson, J. S., and Richardson, D. C. (2010) MolProbity: all-atom structure validation for macromolecular crystallography, *Acta Crystallogr. D Biol. Crystallogr. 66*, 12-–21.
18. Allen, F. H. (2002) The Cambridge Structural Database: a quarter of a million crystal structures and rising, *Acta Crystallogr. B 58*, 380–388.
19. Bruno, I. J., Cole, J. C., Kessler, M., Luo, J., Motherwell, W. D., Purkis, L. H., Smith, B. R., Taylor, R., Cooper, R. I., Harris, S. E., and Orpen, A. G. (2004) Retrieval of

crystallographically-derived molecular geometry information, *J. Chem. Inf. Comput. Sci. 44*, 2133–2144.
20. Afonine, P. V., Grosse-Kunstleve, R. W., Echols, N., Headd, J. J., Moriarty, N. W., Mustyakimov, M., Terwilliger, T. C., Urzhumtsev, A., Zwart, P. H., and Adams, P. D. (2012) Towards automated crystallographic structure refinement with phenix.refine, *Acta Crystallogr. D Biol. Crystallogr. 68*, 352–367.
21. Laskowski, R. A., MacArthur, M. W., Moss, D. S., and Thornton, J. M. (1993) PROCHECK: a program to check the stereochemical quality of protein structures, *J. Appl. Crystallogr. 26*, 283–291.